Simplified Modelling of the F2F MMC-Based High Power DC-DC Converter Including the Effect of Circulating Current Dynamics

Abel A. Taffese* and Elisabetta Tedeschi†
Power Electronics ans Systems Group
Department of Electric Power Engineering
Norwegian University of Science and Technology
Trondheim, Norway
Email: *abel.taffese@ntnu.no and †elisabetta.tedeschi@ntnu.no

***Abstract*—The Front-to-Front Modular Multilevel Converter (MMC) is one of the topologies being considered for high-voltage, high-power, dc-dc conversion. Hence, there is a need for the development of simplified models for such a converter in order to study how it behaves in a large power system. Direct interconnection of two MMC models is one option but it leads to high number of states. Moreover, symmetry of the converter offers further simplification opportunities. The use of this fact to develop a simplified models was reported in literature. However, the resulting models are only applicable when compensated modulation is used. Furthermore, these models neglect the effect of Circulating Current Suppression Controllers (CCSCs), which makes the models inaccurate in the presence of such controllers. This paper proposes a more general simplification approach that captures the effect of CCSC while minimizing the number of states. The proposed model is validated by using time domain simulations and modal (eigenvalue) analyses.**

***Index Terms*—Modular Multilevel Converter, Front-to-Front, dc-dc, F2F, Simplified Model, Modal analysis**

I. Introduction

With the increasing number of installed HVDC links, there is a drive to create a meshed dc grid in order to increase reliability and reduce cost [1]. The high voltage, high power, dc-dc converter plays a vital role in the development of such a grid [2], [3]. In addition to filling the role of the "dc transformer" [4], the converter is also required to provide other services such as power-flow control [2]. The Front to Front (F2F) dc-dc converter composed of two Modular Multilevel Converters connected on the ac side, is one of the promising topologies proposed to meet these requirements [5]. The dc-dc converter is needed when the grid becomes more complex with multiple voltage levels and power-flow paths. This means that it is often studied as part of a large power system. Therefore, it is essential to develop a simplified model of this converter so that it can be used in system level studies. The building block for the converter, i.e. the MMC, is well developed and models of varying level of detail are already available [6]–[13]. However, because of its symmetry, the F2F lends itself to further simplification. This fact was utilized in [14] to develop a simple model of the converter with a single capacitor representing the arm energy dynamics, thus reducing the number of states from 18 to 6. However, as will be shown in this paper, the model is applicable only when using compensated modulation, a special method for calculating the insertion indexes [6]. When using other types of control, such as direct voltage control, there is an uncontrolled interaction between the different harmonic components in the converter, which leads to a poorly damped oscillation at the converter terminals [15]. The existing simplified model of the F2F from [14] fails to accurately capture such modes of oscillation. Additionally, the model neglects the effect of circulating current ripple and the associated suppression controllers. It has been shown that the effect of Circulating Current Suppression Controllers (CCSCs) cannot be neglected because they can interact with external systems [16]. Therefore, the main goal of this paper is to develop a simplified model that can include the circulating current dynamics while keeping the state count to a minimum. The remainder of this paper is organized as follows: A detailed model of the converter is presented in Section II, followed by the proposed simplification in Section III. Validation and analysis of the models are presented in Section IV and Section V, respectively.

II. Detailed Average Modelling

Since the F2F is built from two MMCs, this section will begin by modelling an MMC connected to a stiff voltage source, v_g, on the ac side. The assumptions used to develop the average model are [7]: 1) the insertion indexes are continuous variables, 2) the Sub-Modules are balanced, and 3) the arm capacitance is the same for all the arms. A simplified per-phase equivalent circuit of the F2F, with relevant parameters, is shown in Fig. 1. The following equations can be derived by taking these assumptions into consideration.

$$\begin{aligned} n_u &= n_c - n_s \quad & n_l &= n_c + n_s \\ i_u &= i_c + \frac{1}{2} i_s \quad & i_l &= i_c - \frac{1}{2} i_s \end{aligned} \tag{1}$$

where n_u and n_l are the upper and lower arm insertion indexes, respectively. n_c and n_s are the common-mode (dc) and

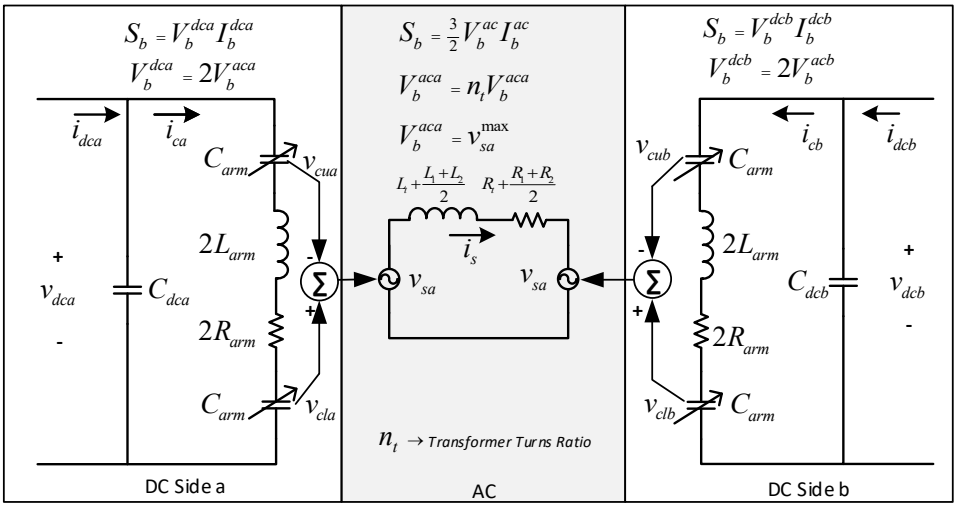

Fig. 1: Per-phase equivalent circuit of the F2F [14]

differential (ac) insertion indexes, respectively. The currents are also shown in (1), where i_c and i_s are the common-mode (circulating) and differential currents, respectively. The differential equations governing dynamics of a leg of an MMC are given by (2), where $v^{\Sigma} = (v_{cu} + v_{cl})/2$ and $v^{\Delta} = (v_{cu} - v_{cl})/2$.

$$\begin{aligned} C_{arm}\frac{\mathrm{d}}{\mathrm{dt}}v^{\Sigma} &= n_c i_c - \frac{1}{2} n_s i_s \\ L_{arm}\frac{\mathrm{d}}{\mathrm{dt}}i_c &= \frac{1}{2}v_{dc} - n_c v^{\Sigma} - n_s v^{\Delta} - R_{arm} i_c \\ C_{arm}\frac{\mathrm{d}}{\mathrm{dt}}v^{\Delta} &= \frac{1}{2} n_c i_s - n_s i_c \\ L_{ac}\frac{\mathrm{d}}{\mathrm{dt}}i_s &= n_s v^{\Sigma} - n_c v^{\Delta} - v_g - R_{ac} i_s \end{aligned} \tag{2}$$

C_{arm}, L_{arm}, and R_{arm} are the equivalent arm capacitance, inductance, and resistance, respectively. L_{ac} and R_{ac} are the equivalent ac side inductance and resistance, respectively. Eq. (2) gives a Steady State Time Periodic (SSTP) model of the MMC, whereas a Steady State Time Invariant (SSTI) model is needed for small signal studies [6]. Dynamic phasor based modelling [8] of the harmonic components is used in order to obtain an SSTI model. The following assumptions are made to simplify the modelling. The quantities i_s, n_s, v^{Δ}, and v_g are assumed to have only a 1st harmonic component, where the harmonic orders are defined with respect to the ac side fundamental frequency. Similarly, i_c, n_c, and v^{Σ} are assumed to have dc and 2nd harmonic components. The harmonic components will be substituted by *phasors* denoted by *boldface* letters with an arrow on top, and the harmonic orders are indicated by the *subscripts*. Since the derivation involves transformation of time domain signals into phasors, a brief description of transforming a product of two time domain signals will be presented here. Given two signals $x(t) = X\cos(k_x\omega t + \phi_x)$ and $y(t) = Y\cos(k_y\omega t + \phi_y)$, the corresponding phasors are $\vec{\mathbf{x}} = X\mathrm{e}^{j\phi_x}$ and $\vec{\mathbf{y}} = Y\mathrm{e}^{j\phi_y}$ rotating at frequencies $k_x\omega$ and $k_y\omega$, respectively. Then, according to the trigonometric angle addition formula, the following is true:

$$\begin{aligned} x(t)y(t) = \frac{1}{2}XY\big[&\cos\left((k_x - k_y)\omega t + \phi_x - \phi_y\right) \\ &+ \cos\left((k_x + k_y)\omega t + \phi_x + \phi_y\right)\big] \end{aligned} \tag{3}$$

The right hand side of (3) can be transformed into two phasor quantities $\frac{1}{2}\vec{\mathbf{x}}\vec{\mathbf{y}}^*$ and $\frac{1}{2}\vec{\mathbf{x}}\vec{\mathbf{y}}$ rotating at frequencies $(k_x - k_y)\omega$ and $(k_x + k_y)\omega$, respectively. Where $(\cdot)^*$ is the complex conjugate operator. If $k_x = k_y$, the real part of the first element is a dc term. Applying phasor transformation, the dc (average) dynamic equations are given by (4), where only the terms resulting in a dc component are included.

$$\begin{aligned} C_{arm}\frac{\mathrm{d}}{\mathrm{dt}}v_0^{\Sigma} &= n_{c0} i_{c0} + \frac{1}{2}\Re\{\vec{\mathbf{n}}_{c2}\vec{\mathbf{i}}_{c2}^*\} - \frac{1}{4}\Re\{\vec{\mathbf{n}}_s\vec{\mathbf{i}}_s^*\} \\ L_{arm}\frac{\mathrm{d}}{\mathrm{dt}}i_{c0} &= \frac{1}{2}v_{dc} - n_{c0}v_0^{\Sigma} + \frac{1}{2}\Re\{\vec{\mathbf{n}}_s\vec{\mathbf{v}}_1^{\Delta *}\} \\ &\quad - \frac{1}{2}\Re\{\vec{\mathbf{n}}_{c2}\vec{\mathbf{v}}_2^{\Sigma *}\} - R_{arm} i_{c0} \end{aligned} \tag{4}$$

where $\Re\{\cdot\}$ is the real part operator. Similarly, the first harmonic components are given by (5).

$$\begin{aligned} C_{arm}\frac{\mathrm{d}}{\mathrm{dt}}\vec{\mathbf{v}}_1^{\Delta} &= \frac{1}{2}n_{c0}\vec{\mathbf{i}}_s + \frac{1}{4}\vec{\mathbf{n}}_{c2}\vec{\mathbf{i}}_s^* - \vec{\mathbf{n}}_s i_{c0} - \frac{1}{2}\vec{\mathbf{n}}_s^*\vec{\mathbf{i}}_{c2} \\ &\quad - \mathrm{j}\omega C_{arm}\vec{\mathbf{v}}_1^{\Delta} \\ L_{ac}\frac{\mathrm{d}}{\mathrm{dt}}\vec{\mathbf{i}}_s &= \vec{\mathbf{n}}_s v_0^{\Sigma} + \frac{1}{2}\vec{\mathbf{n}}_s^*\vec{\mathbf{v}}_2^{\Sigma} - n_{c0}\vec{\mathbf{v}}_1^{\Delta} - \frac{1}{2}\vec{\mathbf{n}}_{c2}\vec{\mathbf{v}}_1^{\Delta *} \\ &\quad - \vec{\mathbf{v}}_g - R_{ac}\vec{\mathbf{i}}_s - \mathrm{j}\omega L_{ac}\vec{\mathbf{i}}_s \end{aligned} \tag{5}$$

The second harmonic part is given by (6).

$$\begin{aligned} C_{arm}\frac{\mathrm{d}}{\mathrm{dt}}\vec{\mathbf{v}}_2^{\Sigma} &= n_{c0}\vec{\mathbf{i}}_{c2} + \vec{\mathbf{n}}_{c2} i_{c0} - \frac{1}{4}\vec{\mathbf{n}}_s\vec{\mathbf{i}}_s - 2\mathrm{j}\omega C_{arm}\vec{\mathbf{v}}_2^{\Sigma} \\ L_{arm}\frac{\mathrm{d}}{\mathrm{dt}}\vec{\mathbf{i}}_{c2} &= -n_{c0}\vec{\mathbf{v}}_2^{\Sigma} - \vec{\mathbf{n}}_{c2}v_0^{\Sigma} + \frac{1}{2}\vec{\mathbf{n}}_s\vec{\mathbf{v}}_1^{\Delta} - R_{arm}\vec{\mathbf{i}}_{c2} \\ &\quad - 2\mathrm{j}\omega L_{arm}\vec{\mathbf{i}}_{c2} \end{aligned} \tag{6}$$

TABLE I: Summary of the considered models

Model	No. of states	Description
Full	22	Full detail average model in *abc* frame suitable for EMT studies
Detailed	18	Detailed SSTI model developed in Section II suited for stability studies
Simple	6	Simplified model proposed in [14] for large scale studies (only suitable for the case of compensated modulation)
Proposed	12	Proposed model based on aggregation of the ripple states for large scale studies

Eqs. (4) to (6) constitute the complete 10^{th} order dynamic phasor model of an MMC leg. The same model can be applied to a balanced three phase system in *dq* domain, where the *d* and *q* components are the real and imaginary parts of the corresponding phasor. The dc voltage dynamics is part of the dc grid dynamic model that includes the cables and dc filter inductances. The model described by (4) to (6) can be extended to the F2F by duplicating all the states except the ac current, because it is common to both sides. This results in a model with 18 states.

III. Proposed Simplification

The complexity of the 18 state model might be acceptable for small scale studies. However, simplification is necessary for the model to be suitable for large scale system studies. The simplifications depend on the type of control employed in the converter, the focus of the study, and the size of the system. In this paper, two simplifying approaches will be compared with the detailed model presented in the previous section. As a starting point, all the ripple components in the arm voltages and the circulating current can be neglected. This model can accurately represent the converter dynamics if compensated modulation is used, as demonstrated in [14]. The resulting dynamic model has only 6 states: $2 \times v_0^{\Sigma}$, $2 \times i_{c0}$, and $\vec{\mathbf{i}}_s$. However, such a model becomes inaccurate when other control methods, such as direct voltage control, are used. Moreover, such a simplification does not include the effect of circulating current suppression controllers. Therefore, an improved simplification approach is proposed here. The approach exploits the symmetry of the converter to reduce the number of the ripple states instead of neglecting them altogether. The simplification is based on the assumption that the two MMCs have the same parameters in per-unit. This is reasonable because the converters are normally designed with similar requirements. Additionally, it is assumed that the circulating current ripples flowing in the two sides, in per-unit, are the same in magnitude but opposite in sign. This implies that $\vec{\mathbf{v}}_1^{\Delta}$, $\vec{\mathbf{v}}_2^{\Sigma}$, and $\vec{\mathbf{i}}_{c2}$ of the two sides can be computed using the values from only one side. Then, the computed values are applied to the two sides after being multiplied by the appropriate sign; this reduces number of states by 6. Therefore, one of the sides is represented with good accuracy while the second one suffers a slight approximation. The approximation is due to the fact that the local couplings between the ripples and the average dynamic states are neglected. This model will be validated and analyzed in subsequent sections. A summary of models covered in this paper is given in Table I.

TABLE II: Selected parameters [15]

Parameters	Value	Parameter	Value
S_b	$1000\,\text{MVA}$	$k_{p,dq}$	$0.192\,\text{pu}$
V_{dc}	$640\,\text{kV}$	$k_{i,dq}$	$2.4\,\text{pu}$
V_{ac}	$320\,\text{kV}$	$k_{p,cc}$	$0.117\,\text{pu}$
C_{arm}	$32.55\,\mu\text{F}$	$k_{i,cc}$	$2.5\,\text{pu}$
$C_{dca} = C_{dcb}$	$193.5\,\mu\text{F}$	f	$50\,\text{Hz}$
L_{arm}	$48\,\text{mH}$	L_t	$58.7\,\text{mH}$
R_{arm}	$1.024\,\Omega$	R_t	$0.512\,\Omega$

IV. Model Validation

Time domain validation of the models in Table I is performed using a test system consisting of the F2F controlled using direct voltage control with circulating current suppression controller implemented in *dq* domain. AC current control in *dq* domain is also implemented. The parameters used for simulation are shown in Table II. Both MMCs are assumed to have the same set of parameters. The dc sides are represented by a voltage source behind a Thevenin impedance (emulating a $10\,\%$ droop). A step change in the dc current from $0.9\,\text{pu}$ to $0.85\,\text{pu}$ is applied at $t = 15\,\text{s}$ in order to excite some of the oscillatory modes in the system. A detailed average model in *abc* frame, developed in accordance with [17] with the same controllers and set of parameters (given in Table II), is used as a benchmark. Figure 2 shows that the detailed 18 state model reproduces the results from the benchmark model with good accuracy. The two simplification approaches are compared using time-domain simulations as shown in Fig. 3. It can be seen that the simple 6 state model fails to accurately capture the oscillations from the detailed model. The improved model, based on the proposed simplification, exhibits good accuracy on side *a* while some modelling error is observed in side *b*. In all the cases considered, the proposed model performs better than the simple 6 state model. Further analysis of the proposed model will be presented in the next section.

V. Analysis

The detailed model is used to perform modal analysis in order to investigate the effectiveness of the simplified models in representing the system dynamics. The time domain simulations can only show response of the system for a given disturbance. Therefore, for proper validation, multiple time domain simulations with different disturbances have to be run so that all the modes are excited, if possible. This is a time consuming process and finding the right combination of inputs (disturbances) is a challenging task. With modal analysis, the validation can be easily done by comparing the eigenvalues and eigenvectors of the different models. Fig. 4 shows eigenvalues of the detailed model. There are 26 eigenvalues in the figure because the test system has 26 states, shown in Table III: 18 states from the detailed converter model, 2 states for dc capacitor dynamics of the two sides, and 6 additional states for controllers. It can be seen that there are 4 pairs of

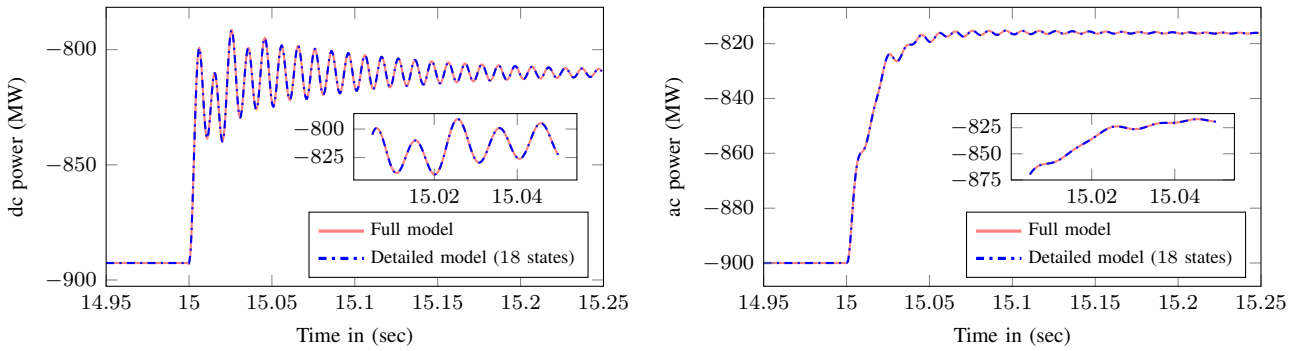

Fig. 2: Time-domain validation of the detailed model: dc power (left) and ac active power (right)

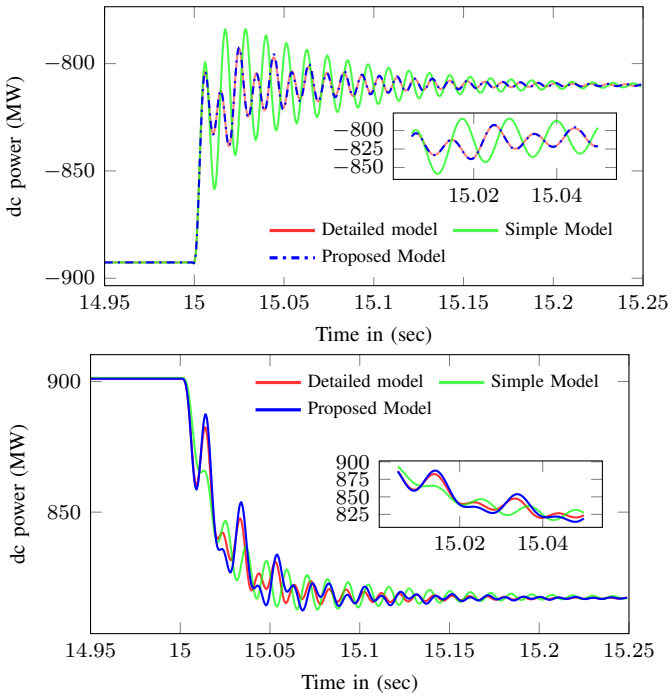

Fig. 3: Comparison of simplified models: dc power of side a (top) and dc power of side b (bottom)

TABLE III: Detailed Model States

Side a	Description	Side b
v_{dca}	dc voltage	v_{dcb}
γ_{da}, γ_{qa}	CCSC states in dq domain	γ_{db}, γ_{qb}
β_{da}, β_{qa}	ac current controller states in dq	—
i_{sd}, i_{sq}	ac current states in dq	—
i_{c0a}	dc common mode current	i_{c0b}
i_{c2da}, i_{c2qa}	Second harmonic circ. current in dq	i_{c2db}, i_{c2qb}
v_{0a}^{Σ}	dc arm voltage	v_{0b}^{Σ}
v_{1da}^{Δ}, v_{1qa}^{Δ}	first harmonic arm voltage ripple in dq	v_{1db}^{Δ}, v_{1qb}^{Δ}
v_{2da}^{Σ}, v_{2qa}^{Σ}	Second harmonic arm voltage ripple in dq	v_{2db}^{Σ}, v_{2qb}^{Σ}

TABLE IV: Effect of the simplification on eigenvalues (Modes)

Detailed Model		Proposed Model	
Mode No.	Value	Mode No.	Value
$1a$	$-747.8 \pm$ j664.4	1	$-755.6 \pm$ j665.9
$1b$	$-774.5 \pm$ j665.9		
$2a$	$-222.7 \pm$ j604.2	2	$-220.75 \pm$ j615.6
$2b$	$-206.4 \pm$ j608.3		
$3a$	$-38.3 \pm$ j654.7	3	$-37.7 \pm$ j654.6
$3b$	$-34.3 \pm$ j634.1		
$4a$	$-16.9 \pm$ j5.96	4	$-17.1 \pm$ j5.93
$4b$	$-20.0 \pm$ j5.62		

eigenvalues, see numbers in Fig. 4, that are located close to each other. These are similar eigenvalues belonging to each of the two sides of the F2F. This can be confirmed by looking at the participation factors for these eigenvalues. Figure 5 shows the participation factors for mode pair 1, where it is visible that Mode 1a is strongly associated to state variables of side a while Mode 1b is to side b. The same pattern is observed for the remaining three mode pairs. This is inline with the fact that the converter has a symmetric structure. It can be noted from Fig. 5 that there are cross couplings between the two sides, but the magnitude of the coupling factors are smaller than those of the local states.

A. *Effect of the Proposed Simplification*

The proposed simplification method replaces the ripple states of side b by those of side a. In doing so, it replaces each pair of eigenvalues in Fig. 4 by a single eigenvalue as shown in Table IV. This can be deduced by examining the eigenvalues and their participation factors. For example, looking at the first pair in Table IV, it can be seen that the eigenvalue from the proposed model is close to that of the detailed model. Moreover, participation factor plot of mode 1, which is shown in Fig. 6, exhibits a similar pattern to the one shown in Fig. 5, where the modes are strongly coupled to the second harmonic circulating current and arm voltage ripples. The 6 state simplified model does not capture any of these modes because it neglects the ripple all together. Comparing the results in Table IV to the time domain plots of Fig. 3, it is evident that the simplified model captures the dynamics of the system side a more accurately that side b. Aside from the inaccuracies in side b, the proposed model can capture the effect of circulating current dynamics and the CCSC. This is

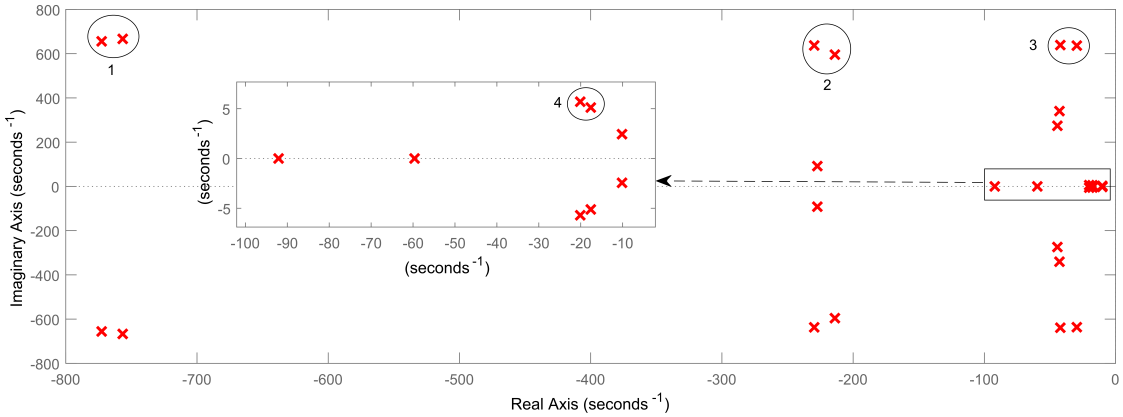

Fig. 4: Eigenvalues from the detailed model

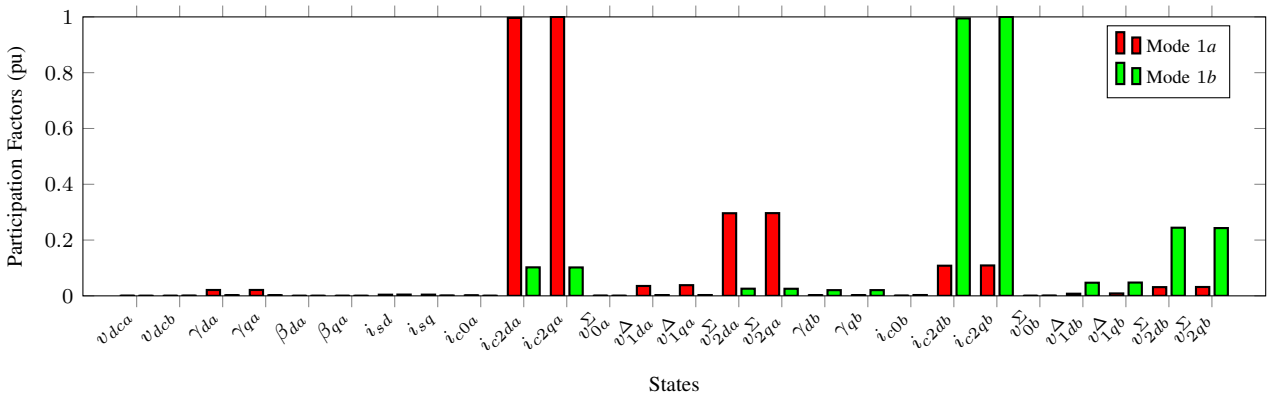

Fig. 5: Participation factors for eigenvalue pair 1

demonstrated by plotting the eigenvalues while changing the proportional gain of the CCSC, $k_{p,cc}$, from 0 to 1. Figure 7 presents the results, which show that the loci of eigenvalues of the two models are in agreement.

VI. Conclusion

This paper presented the development, validation, and analysis of a simplified model of the MMC based F2F dc-dc converter for system level studies. Existing models of such a converter proposed so far are applicable only when compensated modulation is used, which makes it possible to neglect the ripple dynamics. However, when direct voltage control is used, the ripples in the arm voltage and circulating current play an important role in the dynamics of the converter. This is because of the cross-coupling between harmonic components. The approach in this paper is to utilize symmetry of the converter to reduce the number of states. The proposed model results in a reduction in the number of states by 8. This was done by eliminating the ripples and the CCSC from one of the converters. Simulation results comparing the proposed model with the detailed model revealed that the model is able to reproduce the signals from one of the sides with good accuracy, while a slight error is observed from the second side. This was also confirmed by modal analysis which showed that the modes in the proposed model are closer to the ones strongly coupled to one of the sides. The modal analysis also showed that the model preserves the loci of eigenvalues when the circulating current suppression controller gain is varied. This implies that the model correctly represents the effect the controller. Therefore, the proposed model is suitable for representing an F2F, controlled using direct voltage control with CCSC, for large scale system studies where the focus is on controller interaction and stability. The simple 6 state model is not suitable for such a case because it fails to capture even the low frequency modes (as low as $\approx 1\,\text{Hz}$, see Mode 4 in Table IV). The detailed model is the best candidate when the system under study consists of only a few terminals.

References

[1] R. Irnawan, F. M. F. da Silva, C. L. Bak, and T. C. Bregnhøj, "An Initial Topology of Multi-terminal HVDC Transmission System in Europe: A Case Study of the North-Sea Region," in *Ieee International Energy Conference (Enrgycon) 2016*, 2016.

[2] C. Barker, C. Davidson, D. Trainer, and R. Whitehouse, "Requirements of DC-DC Converters to facilitate large DC Grids," *Cigre Sess. 2012*, 2012.

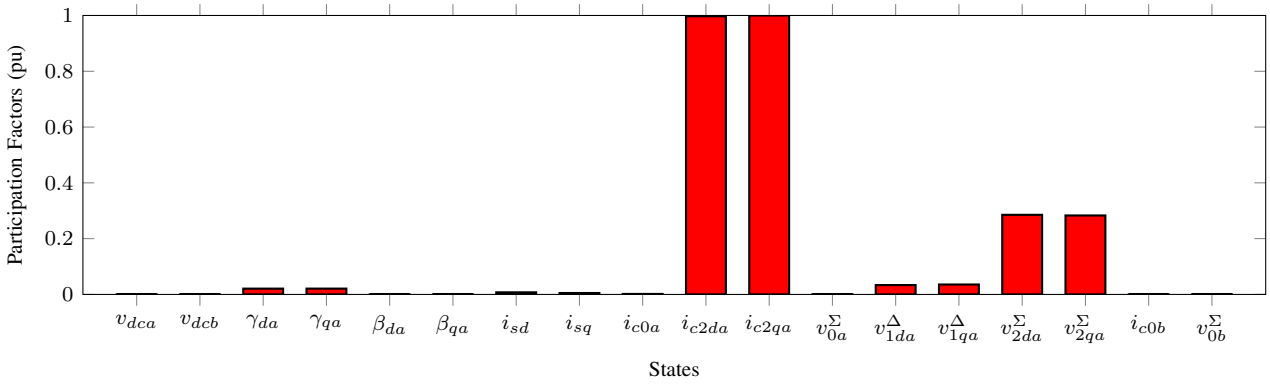

Fig. 6: Participation factors for mode 1 of the simplified model

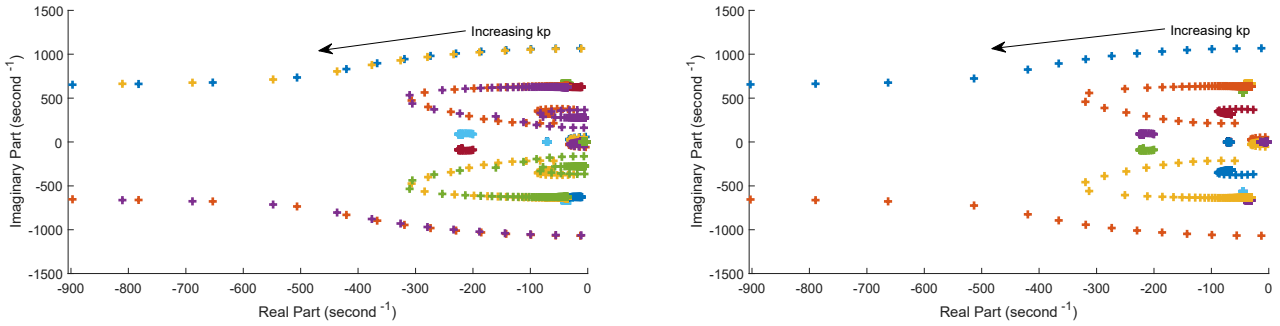

Fig. 7: Effect of CCSC gain on eigenvalues:Detailed model (left) and Proposed model (right).

[3] G. P. Adam, I. A. Gowaid, S. J. Finney, D. Holliday, and B. W. Williams, "Review of dc–dc converters for multi-terminal HVDC transmission networks," *IET Power Electron.*, vol. 9, no. 2, pp. 281–296, 2016.

[4] D. Jovcic and B. Ooi, "Developing DC Transmission Networks Using DC Transformers," *IEEE Trans. Power Del.*, vol. 25, no. 4, pp. 2535–2543, 2010.

[5] A. Schön and M. M. Bakran, "High power HVDC-DC converters for the interconnection of HVDC lines with different line topologies," in *2014 International Power Electronics Conference (IPEC-Hiroshima 2014 - ECCE ASIA)*, May 2014, pp. 3255–3262.

[6] G. Bergna-Diaz, J. A. Suul, and S. D'Arco, "Energy-Based State-Space Representation of Modular Multilevel Converters with a Constant Equilibrium Point in Steady-State Operation," *IEEE Trans. Power Electron.*, vol. PP, no. 99, pp. 1–19, 2017.

[7] L. Harnefors, A. Antonopoulos, S. Norrga, L. Angquist, and H. P. Nee, "Dynamic Analysis of Modular Multilevel Converters," *IEEE Trans. Ind. Electron.*, vol. 60, no. 7, pp. 2526–2537, Jul. 2013.

[8] D. Jovcic and A. A. Jamshidifar, "Phasor Model of Modular Multilevel Converter With Circulating Current Suppression Control," *IEEE Trans. Power Deliv.*, vol. 30, no. 4, pp. 1889–1897, Aug. 2015.

[9] J. Freytes, L. Papangelis, H. Saad, P. Rault, T. V. Cutsem, and X. Guillaud, "On the modeling of MMC for use in large scale dynamic simulations," in *2016 Power Systems Computation Conference (PSCC)*, Jun. 2016, pp. 1–7.

[10] H. Saad, J. Peralta, S. Dennetière, J. Mahseredjian, J. Jatskevich, J. A. Martinez, A. Davoudi, M. Saeedifard, V. Sood, X. Wang, J. Cano, and A. Mehrizi-Sani, "Dynamic Averaged and Simplified Models for MMC-Based HVDC Transmission Systems," *IEEE Trans. Power Deliv.*, vol. 28, no. 3, pp. 1723–1730, Jul. 2013.

[11] U. N. Gnanarathna, A. M. Gole, and R. P. Jayasinghe, "Efficient Modeling of Modular Multilevel HVDC Converters (MMC) on Electromagnetic Transient Simulation Programs," *IEEE Trans. Power Deliv.*, vol. 26, no. 1, pp. 316–324, Jan. 2011.

[12] N. T. Trinh, M. Zeller, K. Wuerflinger, and I. Erlich, "Generic Model of MMC-VSC-HVDC for Interaction Study With AC Power System," *IEEE Trans. Power Syst.*, vol. 31, no. 1, pp. 27–34, Jan. 2016.

[13] R. Wachal and others, "Guide for the development of models for HVDC converters in a HVDC grid," Technical Brochure TB-604, 2014.

[14] A. A. Taffese, E. Tedeschi, and E. C. W. de Jong, "Modelling of DC-DC converters based on front-to-front connected MMC for small signal studies," in *2016 IEEE 17th Workshop on Control and Modeling for Power Electronics (COMPEL)*, Jun. 2016, pp. 1–7.

[15] J. Freytes, G. Bergna, J. A. Suul, S. D'Arco, F. Gruson, F. Colas, H. Saad, and X. Guillaud, "Improving Small-Signal Stability of an MMC with CCSC by Control of the Internally Stored Energy," *IEEE Trans. Power Deliv.*, vol. PP, no. 99, pp. 1–10, 2017.

[16] A. a. J. Far and D. Jovcic, "Circulating current suppression control dynamics and impact on MMC converter dynamics," in *2015 IEEE Eindhoven PowerTech*, Jun. 2015, pp. 1–6.

[17] W. Leterme, N. Ahmed, J. Beerten, L. Angquist, D. V. Hertem, and S. Norrga, "A new HVDC grid test system for HVDC grid dynamics and protection studies in EMT-type software," in *11th IET International Conference on AC and DC Power Transmission*, Feb. 2015, pp. 1–7.